China Geology 9 (2026) 611−623

China Geology

Journal homepage: http://chinageology.cgs.cn
https://www.sciencedirect.com/journal/china-geology

Impact of environmental variables on hydrate formation kinetics in porous media systems and their contribution to CO_2 capture and storage

Jiang Bian[a, b, c,*], Hu-cheng Bai[a], Xue-wen Cao[c], Hong-chao Wang[d], Bo Yu[a, b,*]

[a] *School of Petroleum Engineering*, *Yangtze University*, *Wuhan* 430100, *China*
[b] *State Key Laboratory of Low Carbon Catalysis and Carbon Dioxide Utilization*, *Yangtze University*, *Wuhan* 430100, *China*
[c] *College of Pipeline and Civil Engineering*, *China University of Petroleum* (*East China*), *Qingdao* 266580, *China*
[d] *China Tianchen Engineering Corporation*, *Tianjin* 300400, *China*

ARTICLE INFO

Article history:
Received 10 June 2025
Received in revised form 24 July 2025
Accepted 23 October 2025
Available online 25 February 2026

Keywords:
CO_2 hydrate
Combustible ice
Carbon storage
Hydrate-bearing formatiom
Carbon neutrality
Porous media
Experimental research
Environmental variables
Sediment types (quartz + kaolinite)
Carbon capture, utilization, and storage (CCUS)

ABSTRACT

Global dependence on fossil fuels has led to escalating atmospheric carbon dioxide emissions. The consecutive greenhouse effect poses a serious threat to the human habitat, rendering carbon dioxide abatement a key focus in contemporary research. Hydrate-based CO_2 sequestration offers a promising pathway for carbon capture and storage, though its efficiency is strongly influenced by pressure, salinity, and sediment properties. In this study, the kinetic characteristics and occurrence states of CO_2 hydrates in porous media were systematically investigated under varying pressures (3.0–3.6 MPa), NaCl concentrations (0–3.5%), and sediment types (quartz sand vs kaolinite). Results reveal a non-linear pressure dependence—gas storage capacity increases by 16.3% as pressure rises from 3.0 MPa to 3.3 MPa, but diminishes to 9.4% with further increase to 3.6 MPa. NaCl exhibits dual inhibitory effects: Thermodynamically shifting the phase equilibrium leftward in the *P-T* domain and kinetically suppressing growth, with 3.5% NaCl systems exhibiting persistently slow hydrate formation. Sediment type also plays a critical role, as kaolinite's low-permeability clay structure substantially impedes hydrate formation compared to quartz sand while altering hydrate distribution patterns. Understanding the interplay between pressure-driven efficiency gains and inhibitor-mediated stability control across diverse geological environments is essential for optimizing hydrate-based CO_2 storage strategies.

©2026 China Geology Editorial Office.

1. Introduction

Rising atmospheric CO_2 concentrations are the primary driver of the enhanced greenhouse effect, accounting for over 81% of global greenhouse gas emissions (Ravanchi MT et al., 2011; Kim J et al., 2019; Ahmed R et al., 2020; Jia SJ et al., 2024). Carbon capture, utilization, and storage (CCUS) has emerged as a key strategy for mitigating CO_2 emissions, particularly in fossil-fuel-dependent energy systems where near-term emission reductions are urgently required (Sheng X et al., 2024; Su XN et al., 2024; Hanson E et al., 2025).

Among various CCUS approaches, hydrate-based CO_2 sequestration has attracted increasing attention due to its high selectivity, storage stability, and intrinsic safety. Under suitable temperature and pressure conditions, CO_2 can form solid hydrates, enabling efficient gas separation and reducing leakage risks during geological storage. In marine sediments, especially in deep-sea environments (>300 m), the thermodynamic conditions are favorable for hydrate formation, making them promising sites for large-scale CO_2 sequestration (Prahlad G et al., 2023; Chen HN et al., 2024; Mahmood MN et al., 2024; Pang WX et al., 2024; Cheng CX et al., 2025).

The formation kinetics of CO_2 hydrates in porous media are governed by multiple environmental variables, among which pressure, salinity, and sediment properties play dominant roles. Increasing pressure generally enhances hydrate formation rates and gas storage capacity; however, its quantitative relationship with formation kinetics may vary under different porous structures (Zhang JS and Lee JW,

First author: *E-mail address*: bj@yangtzeu.edu.cn (Jiang Bian).

* Corresponding author: *E-mail address*: bj@yangtzeu.edu.cn (Jiang Bian); yubo@yangtzeu.edu.cn (Bo Yu).

Literary editor: Li-qiong Jia
doi:10.31035/cg2025142
2096-5192/© 2026 China Geology Editorial Office.

Copyright © 2026 Editorial Office of China Geology. Publishing services by Elsevier B.V. on behalf of KeAi Communications Co. Ltd.
This is an open access article under the CC BY-NC-ND License (http://creativecommons.org/licenses/by-nc-nd/4.0/).

2009; Cheng CX et al., 2013). The effect of salinity, particularly NaCl, remains controversial. While some studies report that low concentrations of NaCl can promote hydrate nucleation, higher concentrations significantly inhibit hydrate formation by reducing gas solubility and prolonging induction time (Mekala P et al., 2014; Moeini H et al., 2018; Sun Q et al., 2018; Bian J et al., 2022). In addition, sediment composition, especially clay minerals, introduces complex interactions: Clay surfaces may enhance nucleation by adsorbing gas molecules, whereas excessive clay content can hinder gas diffusion and suppress hydrate growth (Yan KF et al., 2016; Zhang L et al., 2017). These inconsistent findings indicate that the mechanisms governing hydrate formation under coupled environmental conditions remain insufficiently understood.

Despite extensive studies, most existing work has focused on individual factors in isolation, and systematic comparative investigations under unified experimental conditions are still lacking. Furthermore, the occurrence states and spatial distribution characteristics of CO_2 hydrates in clay-containing porous media remain poorly characterized, limiting the accurate evaluation of their storage behavior in natural sediments.

In this study, a comprehensive experimental system was employed to investigate the effects of pressure, NaCl concentration, and sediment type on the formation kinetics of CO_2 hydrates in porous media. Particular attention was given to the comparative analysis of these variables under consistent conditions, as well as to the characterization of hydrate occurrence states in different sediment systems. The findings aim to provide new insights into the coupled effects of environmental variables on hydrate formation and to support the practical implementation of hydrate-based CO_2 sequestration.

2. Experimental system and process

2.1. Experimental section

Fig. 1 shows the experimental setup for CO_2 hydrate formation and decomposition. The system mainly consists of a gas supply unit and a high-pressure reactor. The gas supply unit enables stable CO_2 delivery and real-time monitoring of gas consumption using a mass flow controller. The reactor, with a volume of 100 L, maximum operating pressure of 18 MPa, and minimum temperature of −20°C, serves as the core unit for hydrate formation. The system is equipped with temperature and pressure sensors with appropriate accuracy to ensure reliable measurement and control during experiments. The reactor is connected to a backpressure control unit to regulate hydrate decomposition, and it can be evacuated prior to each experiment to remove residual gases.

The data acquisition system consists of pressure, temperature, and electrical resistance probes, a multi-channel data logger, and a computer for real-time data acquisition, visualization, and storage. A total of 36 probes were installed in the reactor and arranged in three concentric radial circles to capture spatial variations (Fig. 2). Each probe position includes three measurement nodes (top, middle, and bottom),

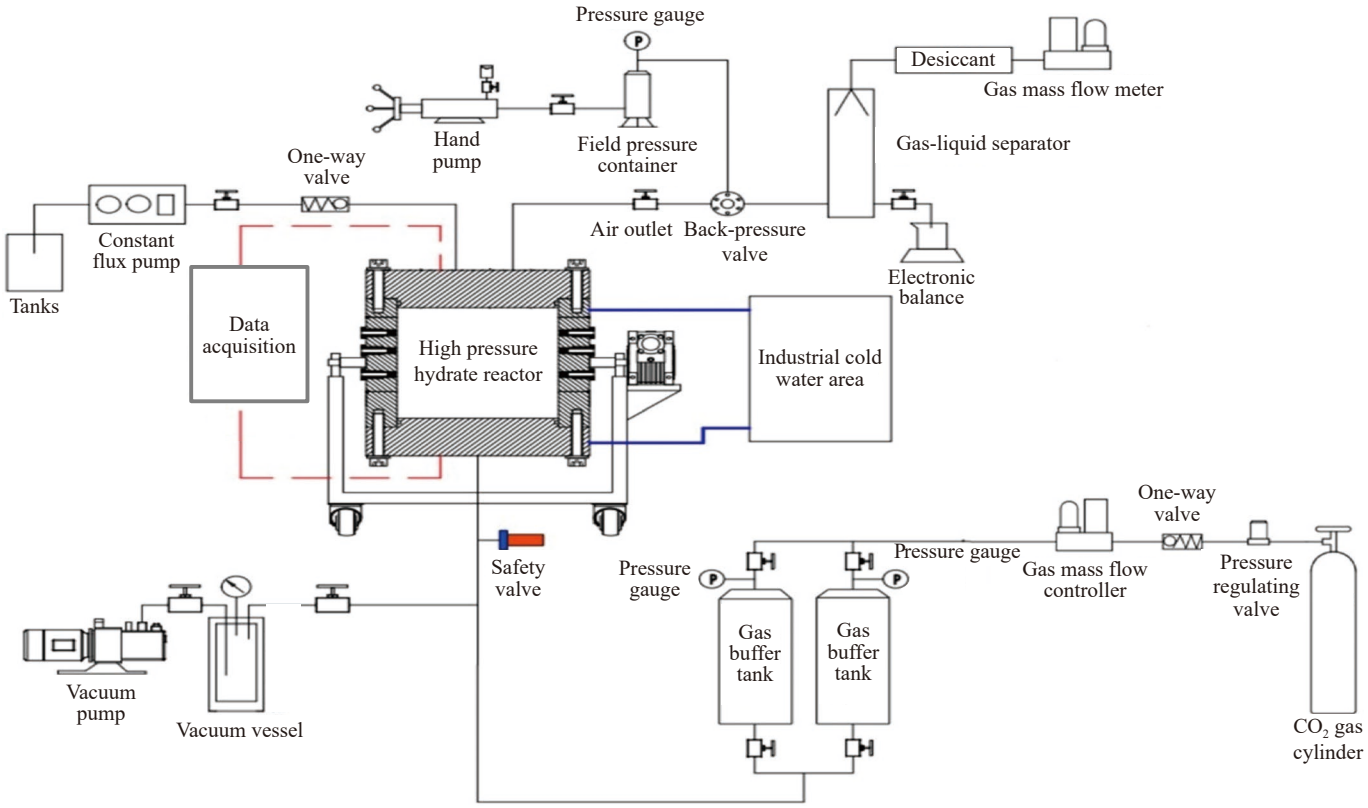

Fig. 1. Process flow chart of the gas hydrate formation and decomposition experiments.

enabling simultaneous monitoring of pressure, temperature, and resistance distribution within the reactor.

Temperature sensors (PT100) have a measurement range of −40°C to 200°C with an accuracy of ±0.1°C. Pressure sensors have a range of 0–25 MPa with an accuracy of ±0.25%. Electrical resistance signals from the resistance probes were also recorded and used as auxiliary indicators for identifying the onset of CO_2 hydrate formation. The cooling system maintains reactor temperature via a circulating coolant bath, allowing precise thermal control during experiments.

2.2. Experimental procedures for the formation of CO_2 hydrates in a porous medium system

(i) Sample preparation. Sediment samples were prepared by sequentially adding a known mass of clean and dry quartz sand (or kaolinite) and deionized water (or 3.5% NaCl solution for salinity experiments) into the reactor (Fig. 3). The mixture was thoroughly stirred to ensure homogeneous distribution and then compacted to avoid air entrapment. The porous medium was fully water-saturated, and the sample height was adjusted to the middle of the reactor observation window where sensors were installed.

(ii) System evacuation and leakage check. Prior to each experiment, the reactor was rinsed and assembled with a new sealing ring. The entire system, including the reactor and gas lines, was tested for airtightness. CO_2 gas was then injected and vented repeatedly three times to remove residual air and ensure a pure CO_2 environment.

(iii) Temperature stabilization and data acquisition. The cooling system and data acquisition system were activated to reach and maintain the preset experimental temperature for at least 1 h before gas injection. Temperature, pressure, resistance, and cumulative gas flow were recorded at 1 min intervals during the experiment.

(iv) Hydrate formation and decomposition. CO_2 was continuously injected into the reactor at a controlled pressure. Hydrate formation was identified by a sudden increase in temperature and resistance. Each experiment was conducted for 20 h, after which gas injection was stopped and the system was shut down. Subsequently, hydrate decomposition was induced by depressurization to atmospheric pressure using a backpressure control system. After complete dissociation, the reactor was cleaned and prepared for the next experimental cycle.

Core experiments investigated the impact of environmental variables on CO_2 hydrate formation in sediment reservoirs. Specifically, the formation process was studied under three pressure conditions (3.0 MPa, 3.3 MPa, 3.6 MPa) using quartz sand to simulate marine sediments. Pure water and a 3.5% NaCl solution were used to mimic pore water. Additional experiments in a kaolinite sediment system assessed the influence of sediment properties. The study also summarized the mechanisms by which sediment type affects CO_2 hydrate formation, and explained differences observed between quartz sand and kaolinite systems.

3. Results and discussion

Given that the environmental conditions of actual sediment reservoirs are variable, factors such as pressure, NaCl concentration, and sediment type can all affect CO_2 hydrate formation and, in turn, its kinetic characteristics. To better optimize carbon capture efficiency and ensure the long-term stability of carbon sequestration, it is crucial to study the effects of different environmental variables on the kinetic characteristics of CO_2 hydrate formation in porous media systems. This provides scientific support for reducing

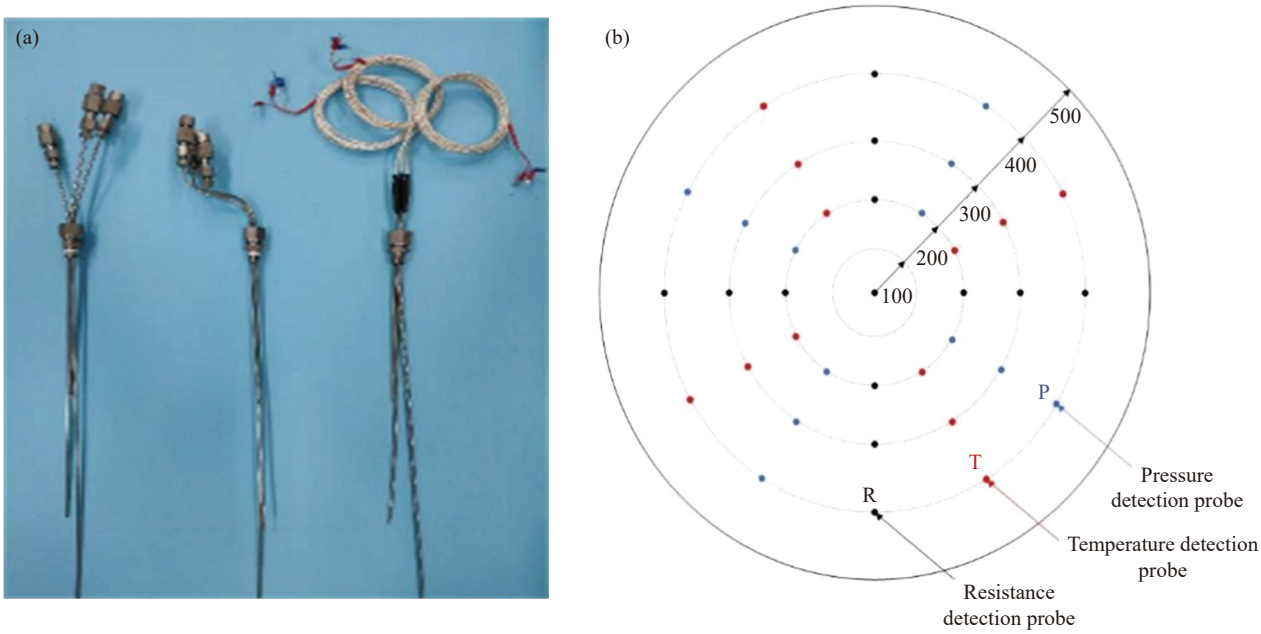

Fig. 2. Schematic diagram of the structure and location distribution of the detection probes. a–Actual structural composition of each detection probe; b–positional layout of each detection probe.

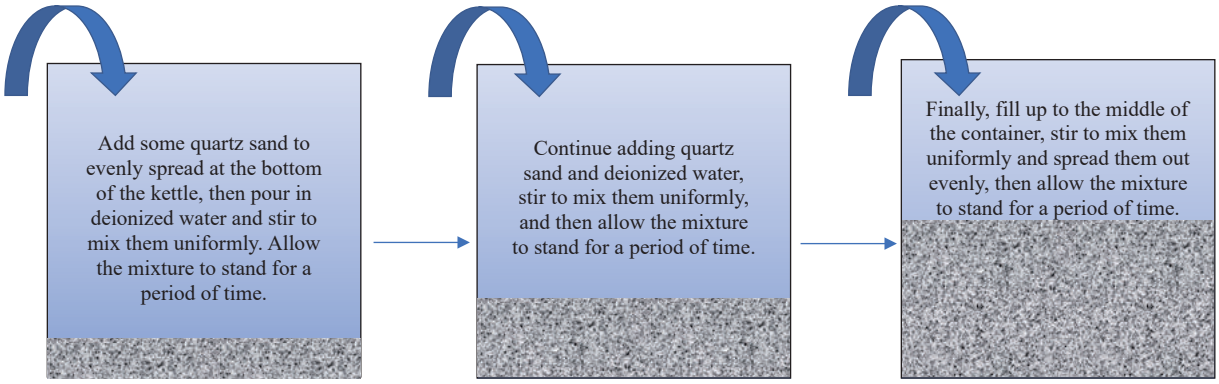

Fig. 3. Preparation methods for the sediment samples.

atmospheric CO_2 concentrations and is an important technical direction for contributing to the "dual carbon" goals and mitigating the greenhouse effect.

3.1. Pressure effect

Pressure is a core thermodynamic variable that regulates the formation process. Higher pressure can enhance the driving force for CO_2 hydrate formation, making it easier for metastable hydrate nuclei to grow, thereby shortening the induction time and accelerating both nucleation and growth rates. This is because high pressure increases the solubility of CO_2 in water, raises the frequency of molecular collisions, reduces the energy barrier required for nucleation, and promotes the diffusion of CO_2 molecules toward the surface of nuclei while stabilizing the hydrate crystal lattice. However, when the pressure exceeds a certain threshold, the solubility of CO_2 in water gradually approaches saturation, the increase in the driving force for formation slows down, and the growth of nucleation and growth rates also weakens accordingly, showing the characteristic of diminishing marginal benefits.

3.1.1. Induction time for CO_2 hydrate formation under different pressures.

The pressure and temperature variation curves during CO_2 hydrate formation at 3.0 MPa, 3.3 MPa, and 3.6 MPa are displayed by Fig. 4 and Fig. 5. At 3 MPa, the temperature of the hydrate reactor was stable at around 6°C. For these conditions, the theoretical phase equilibrium for CO_2 hydrate formation was at 2.5 MPa and 6°C.

By comparing the trends of the different pressure curves in Fig. 4, it can be found that during the formation process of CO_2 hydrates at the three different experimental pressures, the pressure curves exhibit nearly identical pattern. As CO_2 gas was continuously injected, the reaction systems under different pressures quickly reached the theoretical phase equilibrium point for CO_2 hydrate formation, although there were slight differences at specific times; the higher the experimental pressure, the faster the reaction system reached the phase equilibrium point. Then, the pressure continued to increase to the set value and stabilized near that value. By

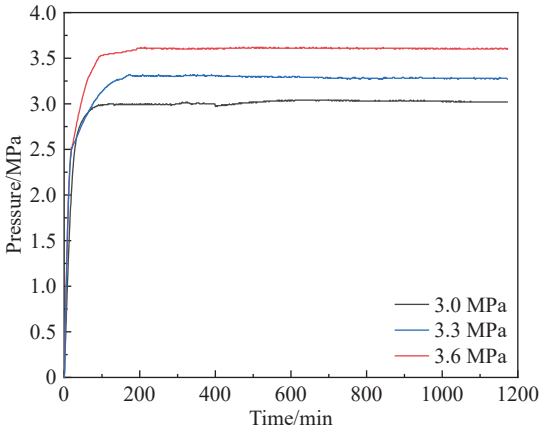

Fig. 4. Pressure curves of the CO_2 hydrate formation process in porous media systems under different pressures.

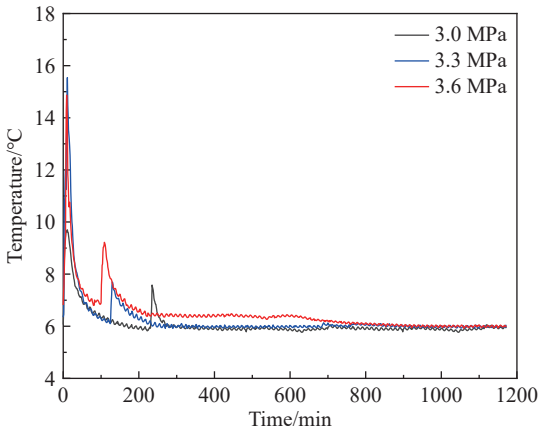

Fig. 5. Temperature curves of the CO_2 hydrate formation process in porous media systems under different pressures.

comparing the changes in the different temperature curves in Fig. 5, a sudden increase in temperature within the reactor can be observed, indicating that at this time, a vigorous hydration reaction occurred between the CO_2 gas and water in the reactor, releasing heat. Moreover, the experimental results show that the higher the experimental pressure is, the earlier the temperature rise begins and the greater the magnitude of the temperature increase. This is because under higher experimental pressures, more CO_2 hydrates are formed in the

reaction system, naturally releasing more heat.

The moment of temperature rise marks the end of induction nucleation and start of CO_2 hydrate formation stage. Induction time is the difference between the end and the beginning of nucleation. Results are in Table 1. As experimental pressure rises from 3.0 MPa to 3.6 MPa, induction time decreases from 156 min to 102 min, showing its decrease with increasing pressure, consistent with Maeda N et al. (2012). This is because higher pressure reduces water surface tension, increases CO_2 solubility, gives more CO_2 per unit volume, enhancing permeability and diffusion, thus implying high supersaturation and driving force for easier metastable hydrate nuclei growth. Experimental results show CO_2 hydrate formation is affected by experimental pressure. The different pressures correspond to the injected gas pressure, with higher pressures providing a greater driving force and influencing the nucleation (induction) time.

3.1.2. Influence of pressure on the kinetic characteristics of CO_2 hydrate formation

Using Eqs. 1, 2, kinetic parameters like cumulative gas consumption, gas conversion rate, and hydrate formation rate during CO_2 hydrate formation experiments can be calculated (Table 2). The table shows that as experimental pressure increases, cumulative gas consumption for CO_2 hydrate formation also increases. This is because higher experimental pressure boosts the driving force for CO_2 hydrate formation, favoring hydrate aggregation and growth, thus increasing consumed CO_2 gas amount.

$$\Delta n_{g,t} = n_{g,0} - n_{g,t} = n_{g,0} - \frac{V}{V_{m,t}} \tag{1}$$

$$C = \frac{\Delta n_g}{n_{g,0}} \times 100\% \tag{2}$$

where, $\Delta n_{g,t}$ is the real-time cumulative consumption of CO_2 gas, $n_{g,0}$ is the cumulative gas intake into the reactor at this moment, $n_{g,t}$ is the amount of remaining CO_2 gas in the reactor at this moment, V is the effective volume occupied by CO_2 gas during the hydration reaction, $V_{m,t}$ is the molar volume of CO_2 gas at this moment, C is the ratio of the total gas consumed to the cumulative gas intake at the end of the experiment for generating CO_2 hydrates and is defined as the gas conversion rate, and Δn_g is the total gas consumed after the experiment is completed.

Table 1. Nucleation start time, nucleation end time, induction time, and temperature rise value under different gas inlet pressures.

Inlet pressure/MPa	Nucleation initiation time/min	Nucleation termination time/min	Induction time/min	Temperature increase/°C
3.0	36	156	120	1.30
3.3	24	127	103	1.53
3.6	19	102	83	2.22

Fig. 6 shows the cumulative gas consumption curves during CO_2 hydrate formation at 3.0 MPa, 3.3 MPa, and 3.6 MPa. The curves start at different points due to different start times of CO_2 hydrate formation under different pressures. All three exhibit distinct formation stages: rapid, stable, and slow formation. After the induction (nucleation) stage ends, CO_2 hydrates form rapidly first and then enter the stable stage. During this stage, the hydrate formation rate reaches a maximum, reaching 0.052 mol/min, 0.067 mol/min, and 0.093 mol/min at the three experimental pressures of 3.0 MPa, 3.3 MPa, and 3.6 MPa, respectively. The CO_2 hydrates basically continue to form stably at these rates. The formation rates subsequently begin to decrease at approximately 600 min, 400 min, and 500 min, respectively, after which they enter the slow formation stage. The overall experimental results show that gas consumption during hydrate formation in a porous medium system is related to pressure. The gas consumption rate (that is, the CO_2 hydrate formation rate) increases with increasing experimental pressure in both stable and slow formation stages. Moreover, as predicted by curve trends, by the end of the reaction, dissolved and adsorbed gaseous CO_2 will be consumed, the CO_2 gas consumption rate will drop to zero, and cumulative gas consumption will stop increasing, causing the curves to flatten at the end.

Comparing hydrate formation rates under different pressures shows that increasing pressure from 3.0 MPa to 3.3 MPa raises the rate from 0.037 mol/min to 0.042 mol/min (a 13.5% increase), while increasing from 3.3 MPa to 3.6 MPa raises it from 0.042 mol/min to 0.045 mol/min (a 7.1% increase). This indicates a diminishing acceleration trend at higher pressures.

A comparison of the final conversion rates of CO_2 gas under different experimental pressures revealed that the final gas conversion rate after the experiment also increased with increasing experimental pressure. The saturation of CO_2 hydrates clearly increases significantly with increasing experimental pressure. This is because higher experimental pressures allow more CO_2 gas to dissolve in water, enabling the formation of more CO_2 hydrates. Overall, under identical conditions, higher experimental pressures favor higher gas conversion rates and hydrate saturations, which is highly important for CO_2 sequestration efforts in engineering practice.

Table 2. Kinetic calculation data under different experimental pressures.

Inlet pressure/MPa	Cumulative gas consumption/mol	Hydrate formation rate/(mol/min)	Gas conversion rate/%	Hydrate saturation/%	Gas storage capacity/(L/L)
3.0	37.34	0.037	84.2	27.88	16.73
3.3	43.44	0.042	87.8	32.44	19.46
3.6	47.52	0.045	90.09	35.49	21.29

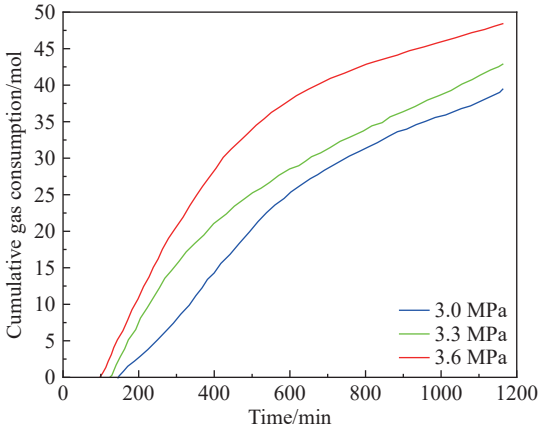

Fig. 6. Cumulative gas consumption of CO_2 hydrates under different pressures in porous media systems.

When the experimental pressure increases from 3.0 MPa to 3.3 MPa, the gas storage capacity rises from 16.73 L/L to 19.46 L/L (a 16.3% increase). When it further increases from 3.3 MPa to 3.6 MPa, the capacity goes from 19.46 L/L to 21.29 L/L (a 9.4% increase). An increase in experimental pressure boosts the driving force for CO_2 hydrate formation, increasing the amount of hydrates and gas storage capacity per unit volume. The experimental pressure significantly impacts gas storage capacity, but the relationship is not linear; as pressure rises, the increase in gas storage capacity diminishes. This suggests that ultrahigh pressures may not be cost effective, indicating that simply increasing the experimental pressure is not an effective means of enhancing the gas storage capacity of sediment systems, which is of great importance for practical engineering applications.

In summary, as experimental pressure increases, the driving force for hydrate formation increases. Higher CO_2 content per unit volume at high pressure enhances CO_2 gas penetration into porous media, reducing induction time, boosting system's CO_2 uptake, and leading to more CO_2 hydrates, higher gas conversion rates, higher hydrate saturations, and greater gas storage capacity of the sediment system.

3.2. NaCl effect

As a common electrolyte in sediments, NaCl mainly plays an inhibitory role. When dissolved in water, its ions form hydration shells with water molecules, disrupting the hydrogen bond network of water and reducing the amount of free water that can participate in the formation of hydrate crystal lattices. At the same time, it lowers the solubility of CO_2 in water, which reduces the thermodynamic feasibility of hydrate formation and shifts the phase equilibrium conditions toward higher pressure and lower temperature. From a kinetic perspective, NaCl reduces the number of water molecules involved in nucleation, raises the energy barrier for nucleation, and prolongs the induction time. It also decreases the diffusion coefficient of CO_2 and even hinders the growth of hydrate nuclei through ion adsorption. This inhibitory effect strengthens with increasing NaCl concentration; at high concentrations (for example, 3.5%), the reduction in formation rate and yield of hydrates becomes more significant.

To understand CO_2 hydrate formation in marine sediment layers for applications such as displacing CH_4 from natural gas hydrates or CO_2 sequestration, this study used quartz sand to simulate marine sediments and pure water and 3.5% NaCl saline water to simulate pore water, then conducted CO_2 hydrate formation experiments.

3.2.1. Induction time for CO_2 hydrate formation in NaCl solutions

NaCl, a thermodynamic inhibitor, affects the equilibrium of hydrate formation by raising the phase equilibrium pressure of CO_2 hydrates at the same temperature, making formation more difficult. Higher pore water salinity shifts the phase equilibrium curve to the left. Fig. 7 shows the effect of 3.5% NaCl on the curve. Below −3°C, it overlaps with that of pure water, but as temperature rises, the phase equilibrium pressure rises and the curve shifts further left. At 6°C, the phase equilibrium pressure of CO_2 hydrates in 3.5% NaCl solution is 3.15 MPa, 0.65 MPa higher than in pure water.

Given that NaCl is abundant in seawater (typical salinity 3.5%), an experiment was conducted on CO_2 hydrate formation in a porous medium with 3.5% NaCl pore water. Using pure water (zero salinity) as a reference. The experimental conditions were 3.6 MPa and 6°C. Fig. 8 shows the temperature variation curves during CO_2 hydrate formation in 3.5% NaCl solution. During the initial gas injection, the reactor temperature rose, but the rise was lower in 3.5% saltwater compared to pure water.

Furthermore, the induction time for CO_2 hydrate formation was significantly longer in 3.5% saltwater, and the heat released at the start of hydrate formation was also reduced (Table 3). This shows that NaCl in pore water inhibits the hydrate nucleation process. The main reason is that when NaCl dissociates in water, it generates a strong electric field that disrupts water molecule clusters, making it harder for them to form the CO_2 hydrate lattice structure, thereby inhibiting formation. The formation process of CO_2 hydrate is a physical phase transition in which gas and water form a cage-like crystal structure under specific conditions. Its core lies in the encapsulation of CO_2 molecules within a cage-like framework constructed by water molecules through hydrogen bonding, resulting in the formation of stable solid crystals. The experimental results indicate that NaCl affects the regular lattice structure of CO_2 hydrates and reduces nucleation, consistent with the findings of Sun Q et al. (2018).

3.2.2. Influence rule of NaCl on the kinetic characteristics of CO_2 hydrate formation

Fig. 9 shows cumulative gas consumption over time during CO_2 hydrate formation in porous media with different salinities. From start to end, cumulative gas consumption in

the NaCl-containing system was 13.55 mol. The curve slope shows the gas consumption rate in the NaCl system was much lower than in the pure water system. The formation rate of CO_2 hydrates without NaCl was about three times that with NaCl. The porous media hydrate formation stage has stable and slow phases, but with NaCl, CO_2 hydrate formation rate was low from the start and stayed near the slow rate, so NaCl-containing systems seem to have only a slow formation phase. Experimental results show NaCl reduces both CO_2 hydrate formation rate and amount. This is because NaCl decreases CO_2 solubility. NaCl is polar like water, while CO_2 is non-polar, and during dissolution, water molecules prefer polar salt ions, forming hydration shells around them, leaving fewer for CO_2, reducing its solubility. This phenomenon is known as the salting-out effect. As time progresses, fewer and fewer dissolved CO_2 molecules are available to form CO_2 hydrates, and the amount of hydrates increases slowly at a basically constant rate until no further change occurs.

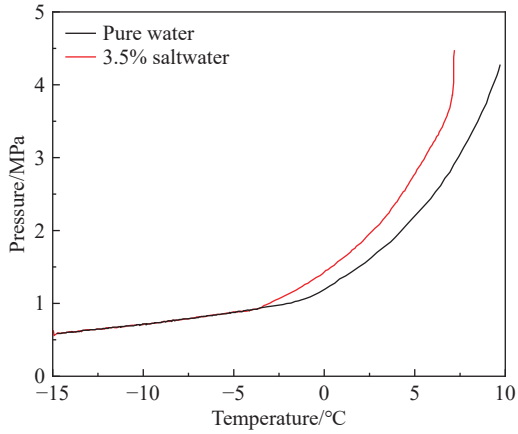

Fig. 7. Phase equilibrium curves of CO_2 hydrates in pure water and 3.5% NaCl solution.

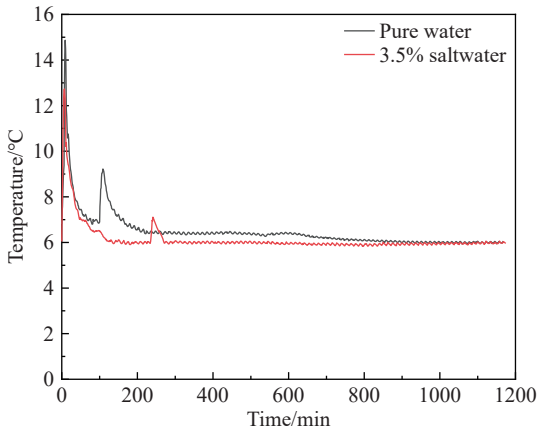

Fig. 8. Temperature curves of the CO_2 hydrate formation process in porous media systems under different salinities.

Table 3. Induction time of the CO_2 hydrate formation process at the different salinities.

Salinity/%	Nucleation initiation time/min	Nucleation termination time/min	Induction time/min	Temperature increase/°C
0	19	102	83	2.22
3.5	107	286	179	1.19

As shown in Table 4, the inhibitory effect of NaCl reduces cumulative gas consumption, hydrate formation rate, gas conversion rate, and hydrate saturation. Regarding the impact of NaCl on the gas storage of sandstone sediment layers, under the same conditions, CO_2 gas consumption affects hydrate formation. In porous media with 3.5% salinity pore water, the highest cumulative gas consumption is 13.55 mol, which is 70% lower than that of pure water. The gas storage capacity per unit volume of the porous media stores 6.07 L of CO_2 gas under standard conditions, which is also 70% lower compared to pure water.

As shown in Table 4, when the salinity increases from 0 to 3.5%, the hydrate formation rate decreases from 0.045 mol/min to 0.014 mol/min, a decrease of about 68.9%; the gas storage capacity decreases from 21.29 L/L to 6.07 L/L, a decrease of about 71.9%.

For porous media systems, after adding a 3.5% NaCl solution, the formation process of CO_2 hydrates primarily involves the following three stages. First, CO_2 gas slowly dissolves in the saline solution. Next, hydrate nuclei form during an induction nucleation phase. Finally, these nuclei grow, and the system transitions into a slow formation stage. Based on previous analysis, the following section summarizes and examines the mechanistic effects of NaCl on each stage of CO_2 hydrate formation:

(i) As shown in Fig. 10, Na^+ and Cl^- ions ionized from NaCl combine with water molecules to form hydrated ions, resulting in a decrease in the number of free water molecules available for hydration with CO_2 gas molecules. This leads to a reduction in the solubility of CO_2 gas, which is the salting-

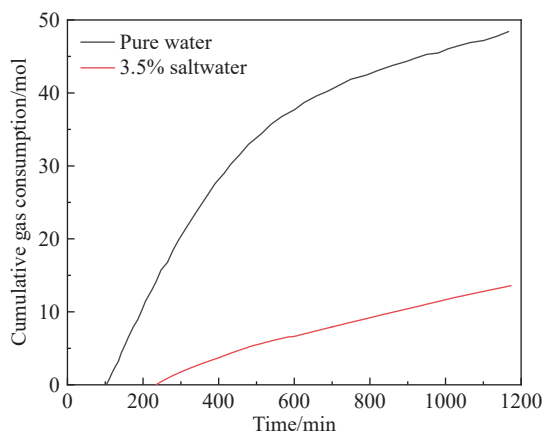

Fig. 9. Cumulative gas consumption of CO_2 hydrates under different salinities in porous media systems.

Table 4. Kinetic calculation data under different salinities.

Salinity/%	Cumulative gas consumption/mol	Hydrate formation rate/(mol/min)	Gas conversion rate/%	Hydrate saturation degree/%	Gas storage capacity/(L/L)
0	47.52	0.045	90.09	35.49	21.29
3.5	13.55	0.014	54.10	10.12	6.07

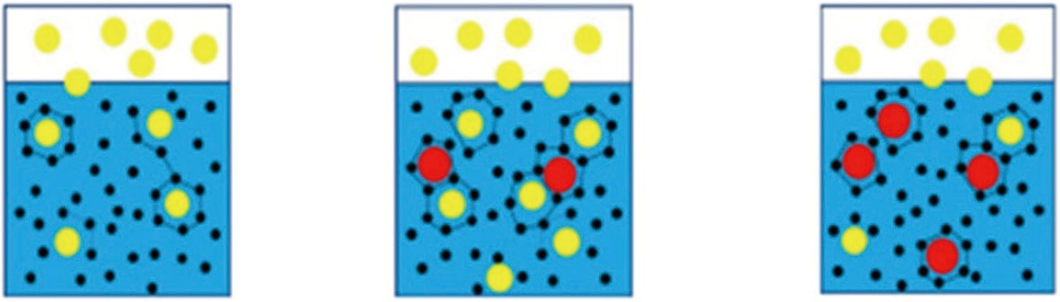

Fig. 10. Dissolution of CO_2 gas at different NaCl concentrations. Yellow dots: CO_2 molecules; red dots: dissociated Na^+ and Cl^- ions from NaCl; black dots: H_2O molecules.

out effect mentioned earlier.

(ii) The water molecules within the reaction system can undergo intense electrostatic interactions with highly hydrophilic Na^+ and Cl^- ions, which significantly disrupts the structure of the water molecules. Therefore, NaCl fundamentally inhibits the nucleation process of CO_2 hydrates. Additionally, relevant research has demonstrated that NaCl reduces the activity of water molecules (Pitzer KS, 2018), leading to a delay in the formation of CO_2 hydrate nuclei, which further impacts the hydrate nucleation process.

(iii) The growth stage of CO_2 hydrate crystals depends on gas dissolution and nucleation. Reduced dissolved CO_2 and inhibited nucleation lower the hydrate formation rate during growth. NaCl does not participate in hydrate formation. As more free water forms hydrates, the salinity of the remaining water increases, further impeding CO_2 dissolution. With fewer water molecules available for hydration shells, a greater driving force is required, highlighting the strengthening inhibitory effect of NaCl on hydrate formation.

In summary, NaCl acts as both a thermodynamic and kinetic inhibitor, making CO_2 hydrate formation more difficult by reducing gas consumption and slowing the overall process. While low concentrations of NaCl may promote hydrate formation, higher concentrations tend to inhibit it. This section uses a 3.5% NaCl solution, and further research is needed to explore the dual effects of varying concentrations.

3.3. Sediment type effect

The influence of sediment type is more complex and is mainly related to particle size, pore structure, and mineral composition. Fine-grained sediments (such as clay) have a large specific surface area and can provide more heterogeneous nucleation sites, which can shorten the induction time in the initial stage of formation. However, due to their small pores and poor connectivity, the pores are easily blocked after hydrate formation, hindering material transfer in the later stage and thus limiting the formation amount. Coarse-grained sediments (such as sandstone) have larger pores and good connectivity, which is beneficial to the diffusion of CO_2 and water, can promote the continuous growth of hydrates, and have a higher overall formation efficiency. Mineral composition also has an impact: The charges on the surface of clay minerals can adsorb water molecules to form an ordered water film, which promotes nucleation to a certain extent. However, if the content is too high, the strong water absorption will dilute the CO_2 concentration.

Currently, most research on CO_2 hydrate formation in porous media focuses on high-permeability sandy sediments like quartz sand, with few studies on clay systems. Drilling and sampling in the South China Sea show hydrate-bearing sediments contain 27% clay. For CO_2 displacement mining of CH_4 and CO_2 sequestration in marine reservoirs, an in-depth study of CO_2 hydrate formation in low-permeability argillaceous clay systems is needed. Kaolinite is a typical clay mineral, so this study investigates CO_2 hydrate formation in kaolinite sediment systems, explores sediment system effects, summarizes the formation mechanism, and explains the differences compared to quartz sand systems.

3.3.1. Induction time for CO_2 hydrate formation in different sediment systems

Using the quartz sand sediment system as a control, the CO_2 hydrate formation experiments were conducted at 3.0 MPa and 6°C. Physical properties of quartz sand and kaolinite are summarized in Table 5. Fig. 11 and Fig. 12 show pressure and temperature change curves during CO_2 hydrate formation in quartz sand and kaolinite systems. As shown, the nucleation time for CO_2 hydrate in kaolinite is significantly longer than in quartz sand. Both systems reached theoretical phase equilibrium at 2.5 MPa and 6°C at about 36 min and entered the induction nucleation stage at the same time. However, the phenomenon of a sharp rise in temperature and vigorous hydrate formation occurred around 285 min later in the kaolinite system than in the quartz sand sediment system and 53 min later than in the pure water system. This indicates that under the same pressure and temperature conditions, the induction nucleation time for CO_2 hydrates in the kaolinite sediment system is longer than that in the quartz sand sediment system, exerting a certain inhibitory effect on hydrate nucleation. Moreover, different sediment types can have a significant effect on the nucleation process of hydrates.

Table 6 summarizes induction time data of two sedimentary systems. In the kaolinite system, CO_2 hydrate

Table 5. Physical properties of the sediment feedstock.

Name	Mesh size	Particle size/μm	Porosity/%	Density/ (g/cm^3)	Thermal conductivity/ (W/(m·K))
Quartz sand	50	300	35	2.4	1.35
Kaolinite	325	45	50	1.6	0.32

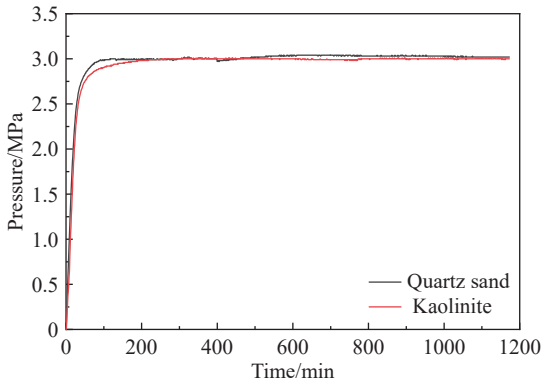

Fig. 11. Pressure curves of the CO_2 hydrate formation process in different sedimentary systems.

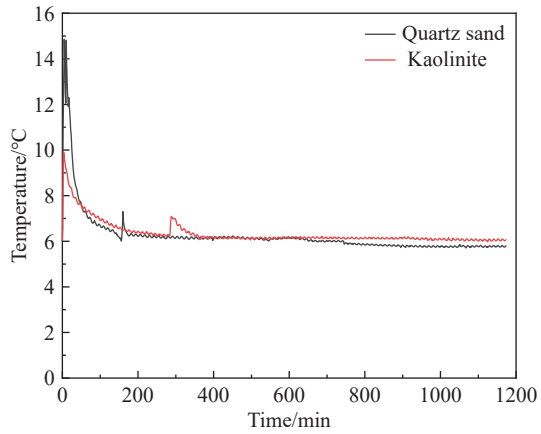

Fig. 12. Temperature curves of the CO_2 hydrate formation process in different sedimentary systems.

formation has a longer induction nucleation time and a 0.22°C lower temperature increase during intense nucleation compared to the quartz sand system. The temperature rise magnitude relates to hydrate amount, suggesting less CO_2 hydrate forms in the kaolinite system.

3.3.2. Influence of sediment type on the kinetic characteristics of CO_2 hydrate formation

Fig. 13 shows the trend of cumulative gas consumption during CO_2 hydrate formation in kaolinite and quartz sand sedimentary systems. In the kaolinite system, the CO_2 hydrate formation process has no distinct stable and slow stages but occurs steadily and slowly at a certain rate.

The curve slopes indicate that from the start of hydrate formation to around 700 min, the gas consumption rate in the kaolinite system is much lower than that in the quartz sand system. After 700 min till the end, the rates of both systems are similar. In the early to mid-stage, the kaolinite system

Table 6. Nucleation start time, nucleation end time, induction time, and temperature rise value during CO_2 hydrate formation in different sedimentary systems.

Sedimentary system	Nucleation initiation time/min	Nucleation termination time/min	Induction time/min	Temperature increase/°C
Quartz sand	36	156	120	1.30
Kaolinite	36	285	249	1.08

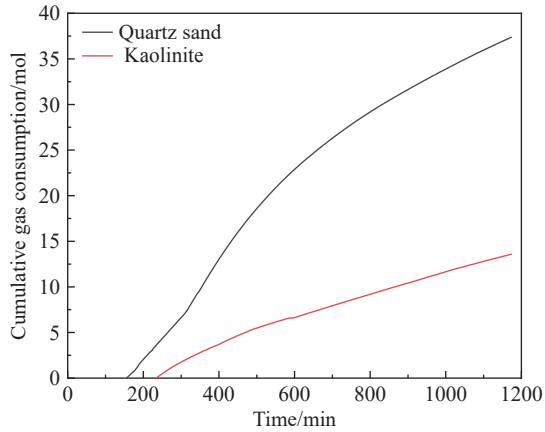

Fig. 13. Cumulative gas consumption during CO_2 hydrate formation in different sedimentary systems.

exhibits lower hydrate formation rate and amount. In the late stage, the rate of the quartz sand system decreases significantly and approaches that of the kaolinite system. At the end of complete formation, the rate of the quartz sand system goes to zero while the rate of the kaolinite system decreases slowly.

Table 7 summarizes the kinetic parameters of the formation process of CO_2 hydrates in both quartz sand and kaolinite sedimentary systems. During the experiments, kaolinite exhibited prominent characteristics of agglomerating upon contact with water, rapidly cementing into distinct mud-like clumps upon mixing. As a result, gas-water contact is impeded, leading to a slower rate of hydrate formation in the kaolinite sedimentary system for CO_2, with lower gas conversion efficiency and saturation. The data in the table indicate that a unit volume of the kaolinite sedimentary system can sequester 9.53 L of CO_2 gas, representing a decrease of approximately 43% in gas storage capacity compared with that of the quartz sand sedimentary system. This is attributed to the strong water absorption capacity of kaolinite, which draws a significant amount of moisture from the system, limiting the availability of free water for hydrate formation. The hydrate formation rate of the quartz sand deposition system is 0.037 mol/min, while in the kaolin system it is 0.024 mol/min, about a 35.1% decrease.

Overall, there are significant differences in CO_2 hydrate formation characteristics in kaolinite and quartz sand systems, due to kaolinite's inherent properties. In quartz sand systems, CO_2 hydrate formation has a rapid and stable stage with many hydrates generated. In kaolinite systems, it's a slow and

Table 7. Kinetic parameters of the CO_2 hydrate formation process in different sedimentary systems.

Sedimentary system	Cumulative gas consumption/mol	Hydrate formation rate/(mol/min)	Gas conversion rate/%	Hydrate saturation/%	Gas storage capacity/(L/L)
Quartz sand	37.34	0.037	84.20	27.88	16.73
Kaolin	21.27	0.024	61.28	11.12	9.53

continuous process. Considering formation rate, amount, gas conversion rate, and gas storage capacity, CO_2 hydrate formation in kaolinite systems is more challenging than in quartz sand systems.

As shown in Table 5, the physical properties of quartz sand and kaolinite sediments (like particle size and porosity) differ. Hydrate formation is due to interfacial tension, capillary phenomena, and diffusion. So, the authors need to discuss their impact on formation kinetics and CO_2 storage. First, sediment particle size affects formation: Smaller particles have larger surface area, enhancing interfacial phenomena and CO_2 adsorption, promoting formation, but also reducing pore size, hindering gas diffusion and inhibiting formation. Hence, the influence of particle size on hydrate formation is uncertain. Particle size affects capillary effect, surface area, porosity, and permeability. Sediment properties are interdependent: Permeability depends on particle size distribution and water saturation, and surface area is determined by porosity and particle size. In the quartz sand system, large grain pore channels aid CO_2 diffusion. In low-permeability kaolinite, as hydrates form, CO_2 permeability decreases with a smaller particle size and higher hydrate saturation, affecting formation and reducing CO_2 storage, outweighing the advantage of the large surface area of small particle size.

3.3.3. Influence of sediment type on the occurrence state of CO_2 hydrates

As shown in Figs. 14a, b, from the perspective of the reactor, in the kaolinite sedimentary system, CO_2 hydrates initially form at the gas-liquid interface, gradually enlarge, and form bulk hydrates that encapsulate the surface of kaolinite, accompanied by cementation with kaolinite clay lumps. This process is similar to the growth of CO_2 hydrates in the quartz sand sedimentary system. Additionally, the hydrates formed at the interface in the kaolinite sedimentary system have thicker bulk structures, whereas in the quartz sand sedimentary system, they form a thinner hydrate film. This is due to the rougher surface of kaolinite, where CO_2 hydrates are more likely to form at the uneven junctions of silt or clay and appear as a covering layer on its surface. Meanwhile, the higher roughness of the kaolinite surface results in greater forces between particles in the sedimentary system, making it difficult for gas to enter the pores between particles, thereby hindering the formation of more CO_2 hydrates.

Figs. 14c–f show the morphological characteristics of quartz sand and kaolinite systems before and after CO_2 hydrate formation and decomposition. Although the formation of CO_2 hydrates cannot be directly observed, the changes in sediment morphology after decomposition, allow us to infer the presence of CO_2 hydrates, as their formation affects sedimentary system morphology.

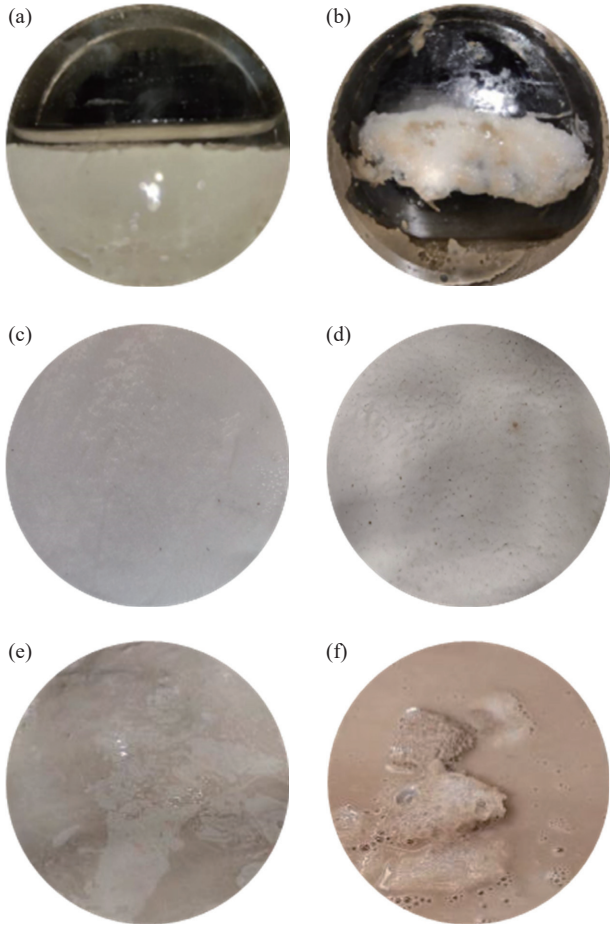

Fig. 14. Macroscopic occurrence characteristics of CO_2 hydrates in different sedimentary systems. a–Formation of CO_2 hydrates at the gas-liquid interface in the quartz sand system; b–formation of CO_2 hydrates at the gas-liquid interface in the kaolinite system; c–quartz sand system before hydrate formation; d–quartz sand system after hydrate decomposition; e–kaolinite system before hydrate formation; f–kaolinite system after hydrate decomposition.

Fig. 14d shows that the decomposed quartz sand system is filled with pores of various sizes caused by the decomposition of hydrates, indicating that the previously formed hydrates mainly occurred in the pores between the quartz sand particles. The quartz sand sedimentary system contained numerous small pores, and the deionized water added before the experiment began was evenly distributed within these pores. However, with the continuous injection of CO_2 gas, some pore-free water was displaced by the CO_2 gas. Throughout the process of CO_2 hydrate formation, ongoing migration of gas and water occurred, coupled with wall-

climbing effects. The "wall-climbing phenomenon" generally refers to a phenomenon where hydrate crystals, during their formation, do not only grow in the main space of the reaction system but also climb upward along the container wall and grow in an attached manner. Therefore, the formed CO_2 hydrates were heterogeneously distributed. Consequently, the pore distribution in the decomposed quartz sand sedimentary system is also uneven. Fig. 14f clearly shows that, unlike those in the quartz sand sedimentary system, the CO_2 hydrates in the kaolinite sedimentary system formed mainly as cemented blocks, and even after the decomposition experiment ended, incompletely decomposed blocks of hydrates containing kaolinite clay lumps remained. This indicates that the heterogeneity of the CO_2 hydrates formed in the kaolinite sedimentary system is even more pronounced.

In the quartz sand sedimentary system, CO_2 hydrates form as particles within the pores of the sand grains, known as pore-filling hydrates. In contrast, in the kaolinite sedimentary system, due to the presence of fine particles, CO_2 hydrates are more randomly distributed as hydrate blocks or nodules. Based on morphological changes in the sediment systems after hydrate decomposition, the microscopic occurrence forms of CO_2 hydrate particles in the pores of the quartz sand and kaolinite sedimentary systems are inferred, as shown in Fig. 15. Quartz sand particles have more nucleation sites between pores than kaolinite does, and hydrates basically nucleate randomly on the surfaces and between the pores of the particles, growing in a suspended manner and ultimately transforming into a skeleton-supported or slightly cemented type. In contrast, the surface of kaolinite is rougher, making it easier for hydrates to nucleate on its surface and grow in an encapsulated manner, ultimately transforming into a cemented agglomerated type.

When kaolinite is mixed with deionized water, it transforms into a muddy clay system with poor permeability. Relevant studies have shown that the permeability of muddy sedimentary systems is several orders of magnitude lower than that of sandy sedimentary systems. This results in restricted diffusion of CO_2 gas and difficult hydrate formation, with this weak gas mass transfer inhibiting the nucleation process of hydrates. Therefore, in the kaolinite system of this experiment, after phase equilibrium conditions for CO_2 hydrate formation were reached, a sharp increase in temperature was captured only after a significant period of time.

Kaolinite's interlayer structure exhibits strong interactions, resulting in high stability. Consequently, when kaolinite comes into contact with water and forms clumps, the bonding forces between its interlayer structures prevent the entry of water molecules. As shown in Figs. 14e, f, kaolinite particles adhere strongly, and the hydrates ultimately formed in a cemented state with the sediment. Under these conditions, the mass transfer of guest molecules is further hindered, resulting in a faster growth rate in the quartz sand sedimentary system compared to the kaolinite system. This finding aligns with the CO_2 hydrate formation pattern shown in Fig. 13. Additionally, most liquid water in the muddy clay system is strongly bound, which is constrained by the sedimentary system and has low water activity, making conversion into gas hydrates difficult. The formation of CO_2 hydrates primarily consumes weakly bound water, as it is easier to form hydrates when the water molecules have weaker binding forces. Together, these factors indicate that kaolinite inhibits the formation of CO_2 hydrates more than quartz sand.

3.4. Error analysis

This study conducted more than five formal replicate experiments, supplemented by multiple preliminary experiments to ensure the sealing integrity of the 100 L large reactor and the accuracy of sensor readings, as well as the reliability of readings from all 36 probes.

Analysis of experimental data indicates that errors introduced by experimental equipment are essentially negligible. Within the experimental system described herein, pressure remains largely uniform across different locations within the reactor vessel. While the industrial chiller maintains a constant temperature in the external cold water bath, significant ambient temperatures and the large volume

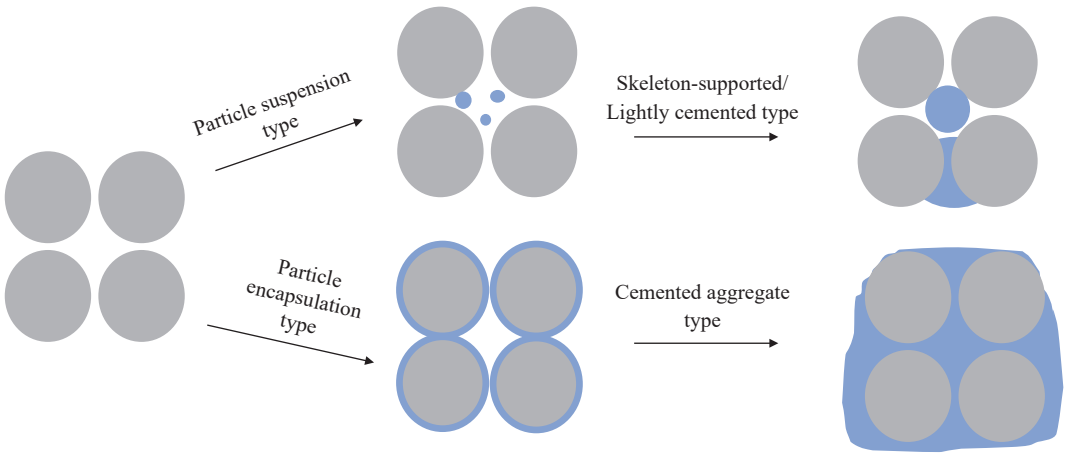

Fig. 15. Microscopic fugitive forms of CO_2 hydrates in quartz sand and kaolinite sedimentary systems.

of the reactor vessel result in temperature variations between probes positioned at different locations. This discrepancy arises from the varying distances of temperature probes from the cold bath: the innermost ring, farthest from the bath, exhibits the highest temperature, followed by the middle ring, with the outermost ring being the coolest.

This paper employs average pressure and average temperature (calculated as the mean values of pressure and temperature data measured at each node by the detection probes) to compute kinetic parameters such as gas consumption. Furthermore, the overall pressure and temperature trend curves for the reaction system are plotted using average pressure and average temperature. To better reflect the statistical significance of experimental data and enhance credibility, the standard deviation σ is calculated for all pressure and temperature data measured at detection probe nodes. Additionally, considering the random nature of hydrate nucleation, standard deviation analysis is performed on the induction times obtained from repeated experiments. The calculation formula is as follows (Eq. 3):

$$\sigma = \sqrt{\frac{\sum_{i=1}^{n}(x_i - \bar{x})^2}{n}} \tag{3}$$

In the formula, x_i represents an individual pressure or temperature measurement, or an induction time obtained from repeated experiments; $\bar{x}$ is the arithmetic mean of the corresponding dataset; and n is the total number of data points.

The standard deviation reflects the dispersion of each measurement data point relative to the mean value. Calculations from Eq. 3 show that the standard deviation of pressure measurement data across different experimental groups remained consistently below 0.01 MPa, indicating minimal pressure variation within the reactor throughout the entire experiment. The standard deviation for temperature measurement data was slightly higher but generally maintained around 0.2℃. This discrepancy stems from the fact that heat transfer non-uniformity is more pronounced than pressure non-uniformity. The standard deviation of induction time measured in repeated experiments was approximately 10.7 min. This stems from the highly random nature of hydration induction times, confirming the stability and reliability of the experimental results. Overall, the calculated standard deviations for both pressure and temperature data were small, indicating that the average data are fundamentally accurate. Therefore, the overall pressure and temperature of the experimental system can be represented by the average values of pressure and temperature at each detection node.

4. Conclusions

In this study, the controlled variable method was employed to investigate the effects of pressure, salinity, and sediment type on the formation kinetics of CO_2 hydrates in porous media, providing theoretical support for the engineering application of hydrate-based CO_2 sequestration and the development of efficient CO_2 storage strategies. The main conclusions are summarized as follows.

(i) Pressure effect: Increasing pressure from 3.0 MPa to 3.6 MPa enhances the hydrate formation rate, gas conversion, and storage capacity, but the enhancement shows diminishing returns. The gas storage capacity increases by 16.3% when the pressure rises from 3.0 MPa to 3.3 MPa, whereas it increases by only 9.4% when the pressure further increases from 3.3 MPa to 3.6 MPa, indicating an optimal pressure range for cost-effective CO_2 storage.

(ii) Salinity effect: NaCl (3.5%) acts as both a thermodynamic and kinetic inhibitor, reducing hydrate formation rate by about 69% and gas storage capacity by about 72% via salting-out and disruption of water hydrogen bonding.

(iii) Sediment type effect: Compared to quartz sand, kaolinite reduces hydrate formation rate by about 35% and gas storage capacity by about 43%. Hydrates form as cemented aggregates rather than pore-filling particles, reflecting poor gas diffusion in low-permeability clay.

(iv) Implications: High-pressure, low-salinity, coarse-grained sediments are optimal for hydrate-based CO_2 storage. Future work should focus on multi-cycle storage efficiency and long-term stability in realistic reservoir conditions.

This study examines the influence of different environmental variables on the kinetic characteristics of CO_2 hydrate formation in porous media systems. The findings enhance the understanding of the fundamental physical properties, formation characteristics, growth patterns, and application potential of CO_2 hydrates, thereby promoting the development of CO_2 sequestration technology toward greater maturity, safety, and reliability. The work lays a theoretical foundation for the application and broader adoption of this technology, providing valuable data and theoretical support for its engineering implementation. This research holds significant strategic value for future environmental protection efforts. In future research, a kinetic model for CO_2 hydrate formation in porous media will be developed, by combining methods such as molecular dynamics simulation.

CRediT authorship contribution statement

Jiang Bian, Bo Yu, and Xue-wen Cao were responsible for the conceptualization of this article; Hu-cheng Bai and Hong-chao Wang undertook the experimental work and the drafting of the manuscript. All authors participated in the discussion of the results and contributed to the manuscript.

Declaration of competing interest

The authors declare no conflicts of interest.

Acknowledgment

This study was supported by the National Natural Science Foundation of China (U21B2087).

References

Ahmed R, Liu GJ, Yousaf B, Abbas Q, Ullah H, Ali MU. 2020. Recent advances in carbon-based renewable adsorbent for selective carbon dioxide capture and separation-a review. Journal of Cleaner Production, 242, 118409. doi: 10.1016/j.jclepro.2019.118409.

Bian J, Wang HC, Yang KR, Chen JW, Cao XW. 2022. Spatial differences in pressure and heat transfer characteristics of CO_2 hydrate with dissociation for geological CO_2 storage. Energy, 240, 122508. doi: 10.1016/j.energy.2021.122508.

Chen HN, Sun YF, Pang WX, Wang ML, Wang M, Zhong JR, Ren LL, Cao BJ, Rao D, Sun CY, Chen GJ. 2024. Quantitative evaluation of hydrate-based CO_2 storage in unsealed marine sediments: Viewpoint from the driving force of hydrate formation and CO_2-water contact ability. Fuel, 376, 132682. doi: 10.1016/j.fuel.2024.132682.

Cheng CX, Zhao JF, Song YC, Zhu ZH, Liu WG, Zhang Y, Yang MJ, Yu XC. 2013. *In-situ* observation for formation and dissociation of carbon dioxide hydrate in porous media by magnetic resonance imaging. Science China Earth Sciences, 56(4), 611–617. doi: 10.1007/s11430-012-4570-5.

Cheng CX, Zhang JH, Wang F, Xiao YQ, Cao Y, Hu WF, Zhu HR, Zhao XC, Hou YF, Yang DX, Zhu SQ, Zhang J, Dong HS, Zhang LX. 2025. Carbon dioxide hydrate formation synergistically enhanced by calcium hydroxide and tetrafluoroethane under low-pressure conditions. Chemical Engineering Journal, 505, 159610. doi: 10.1016/j.cej.2025.159610.

Hanson E, Nwakile C, Hammed VO. 2025. Carbon capture, utilization, and storage (CCUS) technologies: Evaluating the effectiveness of advanced CCUS solutions for reducing CO_2 emissions. Results in Surfaces and Interfaces, 18, 100381. doi: 10.1016/j.rsurfi.2024.100381.

Jia SJ, Yang LB, Han Y, Zhang TF, Zhang XW, Gong PY, Du SY, Chen Y, Ding JB. 2024. Rapid growth of CO_2 hydrate as a promising way to mitigate the greenhouse effect. Materials Today Physics, 48, 101548. doi: 10.1016/j.mtphys.2024.101548.

Kim J, Yu S, Yun ST, Kim KH, Kim JH, Shinn YJ, Chae G. 2019. CO_2 leakage detection in the near-surface above natural CO_2-rich water aquifer using soil gas monitoring. International Journal of Greenhouse Gas Control, 88, 261–271. doi: 10.1016/j.ijggc.2019.06.015.

Maeda N, Wells D, Hartley PG, Kozielski KA. 2012. Statistical analysis of supercooling in fuel gas hydrate systems. Energy and Fuels, 26(3), 1820–1827. doi: 10.1021/ef201965z.

Mahmood MN, Islam MT, Guo BY. 2024. Carbon dioxide hydrate formation in porous media under dynamic conditions for CO_2 storage in low-temperature water zones. Applied Sciences, 14(23), 10860. doi: 10.3390/app142310860.

Mekala P, Busch M, Mech D, Patel RS, Sangwai JS. 2014. Effect of silica sand size on the formation kinetics of CO_2 hydrate in porous media in the presence of pure water and seawater relevant for CO_2 sequestration. Journal of Petroleum Science and Engineering, 122, 1–9. doi: 10.1016/j.petrol.2014.08.017.

Moeini H, Bonyadi M, Esmaeilzadeh F, Rasoolzadeh A. 2018. Experimental study of sodium chloride aqueous solution effect on the kinetic parameters of carbon dioxide hydrate formation in the presence/absence of magnetic field. Journal of Natural Gas Science and Engineering, 50, 231–239. doi: 10.1016/j.jngse.2017.12.012.

Pang WX, Ge Y, Chen MQ, Zhang XH, Wen HY, Fu Q, Lei X, Li QP, Zhou SW. 2024. Large-scale experimental investigation of hydrate-based carbon dioxide sequestration. Energies, 17(13), 3103. doi: 10.3390/en17133103.

Pitzer KS. 2018. Ion Interaction Approach: Theory and Data Correlation. Florida, CRC Press.

Prahlad G, Sadhbhawana D, Sanat K, Avinash P, Asheesh K. 2023. Carbon dioxide sequestration as hydrates in clayey-sandy sediments: Experiments and modeling approach. Chemical Engineering Journal, 475, 146455. doi: 10.1016/J.CEJ.2023.146455.

Ravanchi MT, Sahebdelfar S, Zangeneh FT. 2011. Carbon dioxide sequestration in petrochemical industries with the aim of reduction in greenhouse gas emissions. Frontiers of Chemical Science and Engineering, 5(2), 173–178. doi: 10.1007/s11705-010-0562-1.

Sheng X, Lin SJ, Liang WK, Xie HF, Liu MB. 2024. Optimal long-term planning of CCUS and carbon trading mechanism in offshore-onshore integrated energy system. Applied Energy, 379, 124983. doi: 10.1016/J.APENERGY.2024.124983.

Su XN, Liu PF, Mei YD, Qiu JX. 2024. The impact of carbon capture, utilization, and storage (CCUS) projects on environmental protection, economic development, and social equity. Journal of Cleaner Production, 482, 144218. doi: 10.1016/J.JCLEPRO.2024.144218.

Sun Q, Tian H, Guo XQ, Liu AX, Yang LY. 2018. Solubility of CO_2 in water and NaCl solution in equilibrium with hydrate. Part II: Model calculation. The Canadian Journal of Chemical Engineering, 96(2), 620–624. doi: 10.1002/cjce.22939.

Yan KF, Li XS, Chen ZY, Xia ZM, Xu CG, Zhang ZQ. 2016. Molecular dynamics simulation of the crystal nucleation and growth behavior of methane hydrate in the presence of the surface and nanopores of porous sediment. Langmuir, 32(31), 7975–7984. doi: 10.1021/acs.langmuir.6b01601.

Zhang JS, Lee JW. 2009. Enhanced kinetics of CO_2 hydrate formation under static conditions. Industrial and Engineering Chemistry Research, 48(13), 5934–5942. doi: 10.1021/ie801170u.

Zhang L, Xu SD, Li X, Zhang Y, Yang RH, Qian OY, Ren SR. 2017. Reaction kinetic characteristics and model of methane hydrate formation in porous media. Energy and Fuels, 31(8), 8548–8559. doi: 10.1021/acs.energyfuels.7b00958.